TRANSNAV
http://www.transnav.eu

the International Journal
on Marine Navigation
and Safety of Sea Transportation

Volume 12
Number 3
September 2018

DOI: 10.12716/1001.12.03.09

Dredging Volumes Prediction for the Access Channel of Santos Port Considering Different Design Depths

L.M. Pion
Hydraulic Technological Center Foundation, Sao Paulo, Brazil

J.C.M. Bernardino
University of Sao Paulo, Sao Paulo, Brazil

ABSTRACT: Santos is the most important Brazilian port, handling about 114 million of tons in 2016. In 2010, there was a great capital dredging in order to deepen the Access Channel to 15m deep (Chart Datum - CD). This depth was not achieved, due to inefficiency on dredging procedures. As deepening and maintaining design depths are indispensable, this study presents an analysis of sediment deposition in Santos Port Access Channel and an annual dredging volumes prediction, considering current bathymetric survey and design depths of 15, 16 and 17 m (CD).A numerical hydrodynamic and morphological model was developed for the interest area, by using Delft3D®, calibrated with waves, currents and water level data measured within Santos Port adjacen-cies. Sediment transport model was calibrated with suspended sediment data and historic series of dredged volumes from Santos Port Access Channel. Two different scenarios were simulated for each design depth, according to the regional environmental characteristics. For current bathymetric scenario, the model estimates that it would be necessary to dredge an annual average of about 4,325,000 m³ from Santos Port access chan-nel to maintain current depth condition. Regarding design depths of 15, 16, 17 meters, it would be an in-crease of 15%, 55%, and 80%.

1 BACKGROUND

Officially inaugurated on February 2nd, 1892, Santos Port is the most important port in Latin America, being responsible for 25% of the Brazilian balance of trade. Once it is located in an estuarine area, naturally deep, the first capital dredging was performed only in 1964, 72 years after the port inauguration. In this time, it was intended to establish a design depth of 14.8 m (CD) in the access channel. However, the design depth was never reached, due to the inefficiency of dredging proceedings, and the access channel depth was maintained in about 12.5 m (CD).

In 2010, another capital dredging was made in Santos Port, in order to deepen the access channel to a design depth of 15 m (CD). Once more, again due to the inefficiency of dredging procedures, the design depth was never reached. In July 2017, it was established a maximum operational draft in Santos Port of 12.6 m, after depths lower than 14 m were observed in bathymetric surveys.

Considering an expected enlargement of commercial vessels all around the world, associated with the role of hub port currently played by the Port of Santos, it is indispensable to deepen and maintain design depths. In this context, the main goal of this study is to analyze sediment deposition in Santos Port Access Channel and predict annual maintenance dredging volumes, considering current bathymetric survey and design depths of 15, 16 and 17 m (CD), based on a numerical hydrodynamic and morphological model.

2 STUDY AREA DESCRIPTION

Santos Port is located in Brazilian southeastern coast, (Figure 1). The city of Santos is located at Sao Vicente Island, within a very complex estuarine system, where there are more than 60 river outfalls. The Santos Port is situated in both margins of the estuary outfall. The Santos Port area is shown in Figure 2. Its access channel is divided into four different areas, such as illustrated in Figure 3.

Figure 1. Location of Santos Port (Google Earth).

Figure 2. Santos Port Area (Google Earth)

Figure 3. Scheme of Santos Port Access Channel (Google Earth)

This area's climate characteristics are well defined by two different seasons: a rainy period, usually between spring and summer (from October to March), during which around 70% of annual rainfall takes place; and a dry one, between April and September. These periods are generally designated as summer and winter, respectively. Also, winter period is known for high significant wave heights, due to the occurrence of cold fronts generated in the oceanic area (storm surges), which do not frequently occur in the summer period.

The tide is semidiurnal, with amplitudes varying between 0.27m, in the neap tide, and 1.23m, in spring tides. However, considering meteorological effects, the water level can reach up to 1.83 m. Maximum flow speed is about 1m/s along the access channel, near the estuary outfall, but it does not exceed 0.5 m/s in most of Santos bay.

In Area I, bottom sediment is basically sand (70%) and its fraction decreases inward the estuary. In Area II, the sand fraction is about 50%, while in Area III it is about 40%. In Area IV, the most inner, bottom sediment is basically fine sediment (silt and clay).

For areas which are not subject to wave action (II, III and IV), sediment deposition is directly related to rain seasonality, due to higher river flow and, consequently, higher total sediment transport load. Hence, sediment deposition in Areas II, III and IV is expected to be more intense in the summer period.

As Area I is exposed to wave action and located in an area characterized by low current speeds. Its sediment deposition pattern is associated with wave climate. Generally, in the winter period, when waves are higher, sediment deposition is more intense in Area I. In periods characterized by higher waves, sediment is removed from the beaches and tends to settle at the channel area.

3 DATABASE

For the study development, waves, currents, and water level measured within Santos Bay and Estuary were used. Also, for model calibration and boundary conditions, waves, wind, and tide data were extracted from global models, WaveWatch III, NCEP/CFSR and TPXO, respectively. Figure 4 illustrates all measurement and global model points used for model boundaries and calibration.

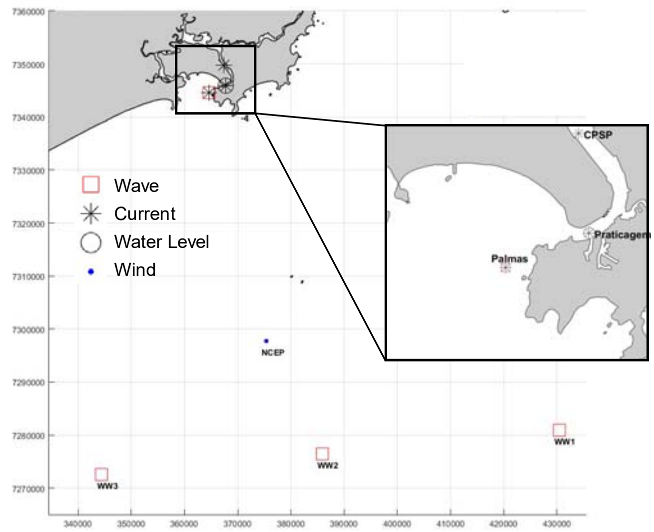

Figure 4. Measurement and global model points (UTM 23S – WGS 1984)

Also, bed representation was based on a bathymetric survey realized in March 2016 at the

Santos Port Access Channel and Nautical Charts from Brazilian Navy data (CHM, 2016). Sediment characteristics and river flow used in modeling were obtained from the Study of Environmental Impact of the last capital dredging (Fundação Ricardo Franco, 2008).

4 MODEL REPRESENTATION

4.1 *Model Background*

Delft3D hydrodynamic module simulates non-uniform flows and transport phenomena using water level variation, river discharges or meteorological forcing variables, including density gradient effects, calculated from salinity and temperature distribution. This model can be used to predict flow patterns in shallow regions, coastal, estuarine or lake areas (Deltares, 2014). In this case, numerical modeling is based on the continuity equation, the momentum conservation equation (Navier-Stokes) and the transport equations solution.

The model solves Navier-Stokes equations for an incompressible fluid, considering the Boussinesq approximation, in which fluid density is considered to be constant, except for the baroclinic term, which represents flow variations due to vertical density gradients. Moreover, the Boussinesq approximation does not account for vertical flow acceleration, considering hydrostatic pressure. This hypothesis is valid when the horizontal extension is much larger than flow depths (Deltares, 2014).

Navier-Stokes equations are simplified using Reynolds average, which means deriving these equations from variables decomposition in time average and turbulent components, which are equal to zero when integrated on time by definition (Versteeg and Malalasekera, 2007). Numerical simulations are performed through the finite differences method, and space is divided into cells from a computational grid. Delft3D uses orthogonal curvilinear coordinates. In this case, the flow speed is calculated according to the orientation of grid cell faces. The water level is calculated at the center of the cells (Deltares, 2014).

The Delft3D wave module (SWAN) is a spectral wave model, able to reproduce wave propagation, wave generation by wind and non-linear wave interactions and dissipation in deep, intermediate and finite waters (Deltares, 2014). The model solves the energy balance equation for wave energy transport, including waves generation by wind, non-linear wave interactions, bottom friction, depth-induced breaking, and energy dissipation by whitecapping.

The two modules shall be coupled in order to accurately represent hydrodynamic conditions at the interest area. The coupling accounts several important processes due to wave-current interaction, such as enhancement of vertical mixing due to wave-induced turbulence and enhancement of the bed shear stress by waves. For this case, Fredsoe (1984) wave-current interaction model was used.

In order to properly represent sediment transport, it was necessary to consider fine sediment and sand transport, due to bed material characteristics. Hence, it was necessary to use two different equation for sediment transport. Generally, transport of suspended sediment is defined by the advection-diffusion equation for suspended sediment concentration, as shown in Equation (1):

$$\frac{\partial c}{\partial t}+\frac{\partial uc}{\partial x}+\frac{\partial vc}{\partial y}+\frac{\partial (w-w_s)c}{\partial z}-\frac{\partial}{\partial x}\left(\varepsilon_x\frac{\partial c}{\partial x}\right)-\frac{\partial}{\partial y}\left(\varepsilon_y\frac{\partial c}{\partial y}\right)-\frac{\partial}{\partial z}\left(\varepsilon_z\frac{\partial c}{\partial z}\right)=0 \quad (1)$$

where:
c – suspended sediment concentration (kg/m³);
u, v and w – flow velocity components, in directions x, y, and z respectively (m/s);
w_s – settling sediment speed;
ε_x, ε_y e ε_z – eddy diffusivity in directions x, y and z.

For fine sediment erosion and deposition, the Partheniades-Krone formulations (Partheniades, 1965) were used, as described below in Equations (2) and (3). The model considers that fine sediment is only transported in suspension.

$$E = M\ S_e \quad (2)$$

$$D = w_s\ c\ S_d \quad (3)$$

where:
E – erosion flux (kg/(m² s));
M – erosion parameter (kg/(m² s));
D – deposition flux (kg/(m² s));
w_s – settling sediment speed;
c – fine sediment concentration near bottom;
S_e – erosion step function;
S_d – deposition step function.

The step functions are calculated as exposed in Equations (4) and (5).

$$S_e=\begin{cases}\left(\dfrac{\tau}{\tau_{cre}}-1\right), when\,\tau>\tau_{cre}\\ 0, when\ \tau\le\tau_{cre}\end{cases} \quad (4)$$

$$S_e=\begin{cases}\left(1-\dfrac{\tau}{\tau_{crd}}\right), when\,\tau<\tau_{crd}\\ 0, when\,\tau\ge\tau_{crd}\end{cases} \quad (5)$$

where:
τ – bed shear stress;
τcre – critical erosion shear stress;
τcrd – critical deposition shear stress.

Non-cohesive sediment transport was computed by Van Rijn (1993) formulation. Bedload transport and suspended-load are distinguished by a reference height, above which sediment transport is considered as suspended-load and below which sediment transport is considered bedload. The interaction between bedload and suspended transport is computed by using a reference concentration, calculated as shown in Equation (6), which is imposed in the water column at the reference height:

$$c_a = 0.015\rho_s \frac{D_{50} T^{1.5}}{a D_*^{0.3}} \quad (6)$$

where:
c_a – sediment concentration at reference height;
ρ_s – sediment specific density;
T – non-dimensional bed shear stress;
a – reference height;
D_{50} – median sediment diameter;
D* - non-dimensional particle diameter.

Bedload transport rate is computed as (7):

$$S_b = 0.006\rho_s w_s D_{50} M^{0.5} M_e^{0.7} \quad (7)$$

where:
S_b – bedload transport (kg/(m s));
M – sediment mobility number;
M_e – excess sediment mobility number.

M and Me are non-dimensional parameters, given by (8), (9) and (10):

$$M = \frac{v_{eff}^2}{(s-1) g D_{50}} \quad (8)$$

$$M_e = \frac{(v_{eff} - v_{cr})^2}{(s-1) g D_{50}} \quad (9)$$

$$v_{eff} = \sqrt{v^2 + U^2} \quad (10)$$

where:
V_{cr} – critical flow speed for particle motion, based on shields curve;
V – depth-averaged speed;
U – near-bed peak orbital velocity, due to wave action, based on significant wave height.

4.2 *Model description*

Two different grids were used to perform the simulations for the interest area. Figure 5 presents the grid used for wave propagation simulation and Figure 6 shows the grid for flow and sediment transport simulation. At the interest area, both grids were refined to a resolution of about 20 m. As already mentioned, wave and wind boundary conditions were forced with WaveWatch III and NCEP/CFSR data, respectively. Also, flow model boundary was forced by TPXO global tide model harmonic constituents, complemented with NCEP/CFSR data for mean sea level elevation, in order to adequately represent meteorological effects in water level at the interest area. Bottom roughness was set considering bed material characteristics and adjusted according to hydrodynamic model results' precision. In addition, river flow data and total load were inserted in the model domain as sources, considering each outfall location.

For sediment transport simulation, two different sediment fractions were considered: a fine one and a coarser one (sand), which availability and positioning within model domain were defined according to the proportion of sediment data presented in the Study of Environmental Impact of the Access Channel Capital Dredging collected at the interest area.

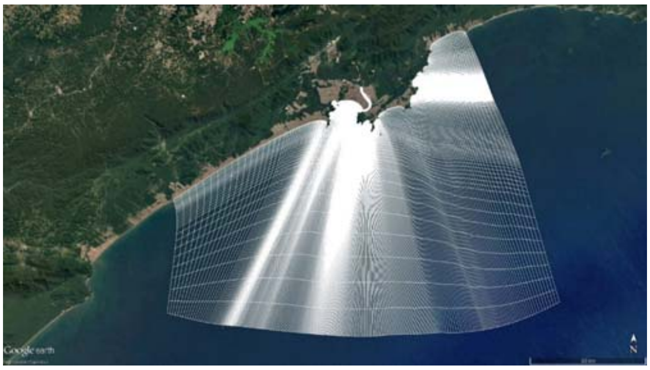

Figure 5. Wave grid

Figure 6. Flow and Sediment transport grid

4.3 *Model accuracy obtained*

The accuracy of waves representation by the model was evaluated considering the comparison between model results and wave measurements at Palmas (Figure 4) point. RMSE (Root Mean Squared Error) index was used as a statistical indicator of model accuracy. The closer its value is from zero, better is model accuracy. Also, Figure 8, Figure 9 and Figure 10 show the comparison between model results and field data for current speeds at Praticagem, Palmas and CPSP points (Figure 4), respectively. Finally, Figure 11 presents water level comparison between field measurements and model results. The comparison between field data and model results reveals overall model's good representation of the hydrodynamic field at the interest area.

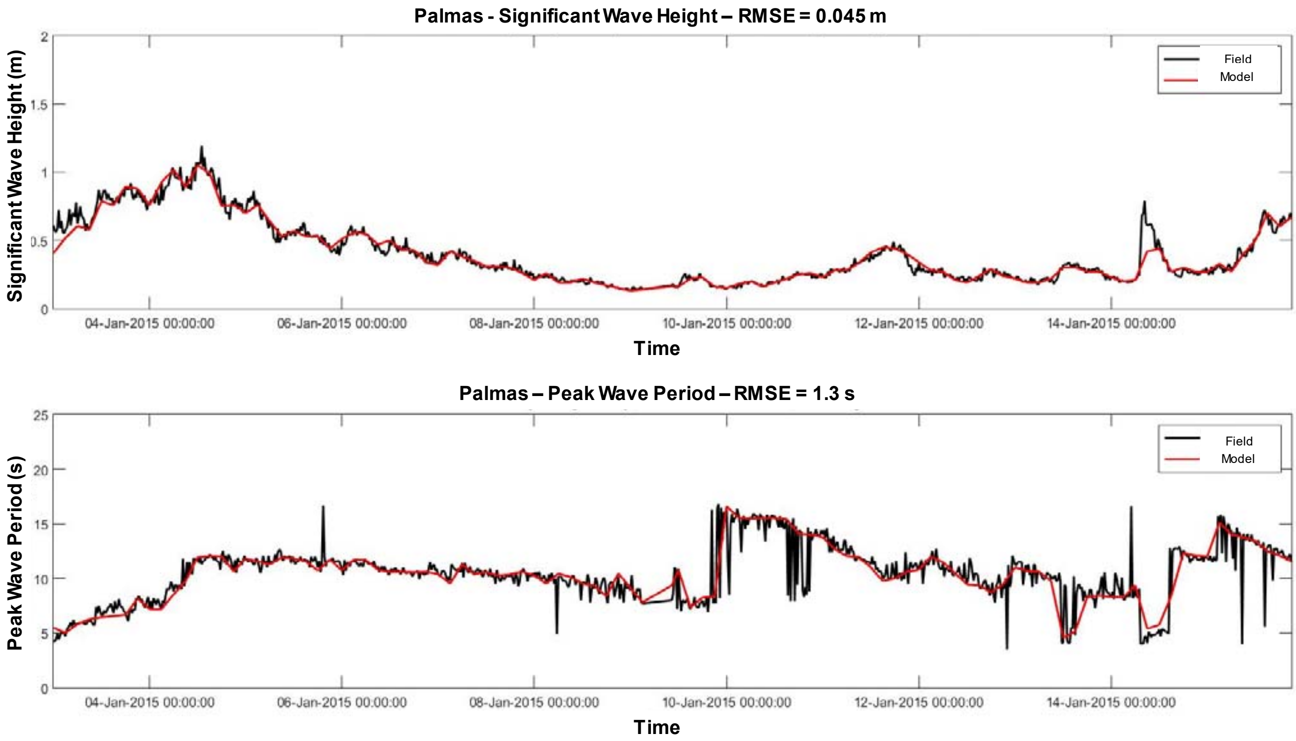

Figure 7. Field X Model Comparison - Waves – Palmas

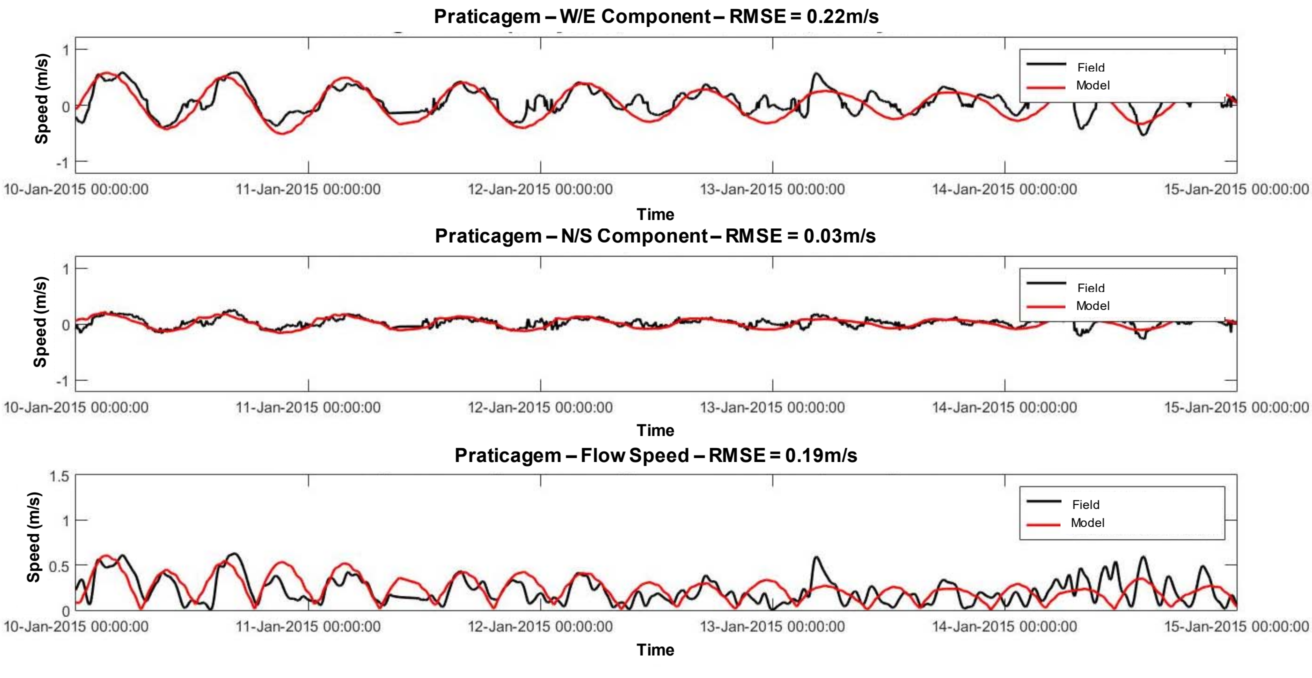

Figure 8. Field X Model Comparison - Current Speed – Praticagem

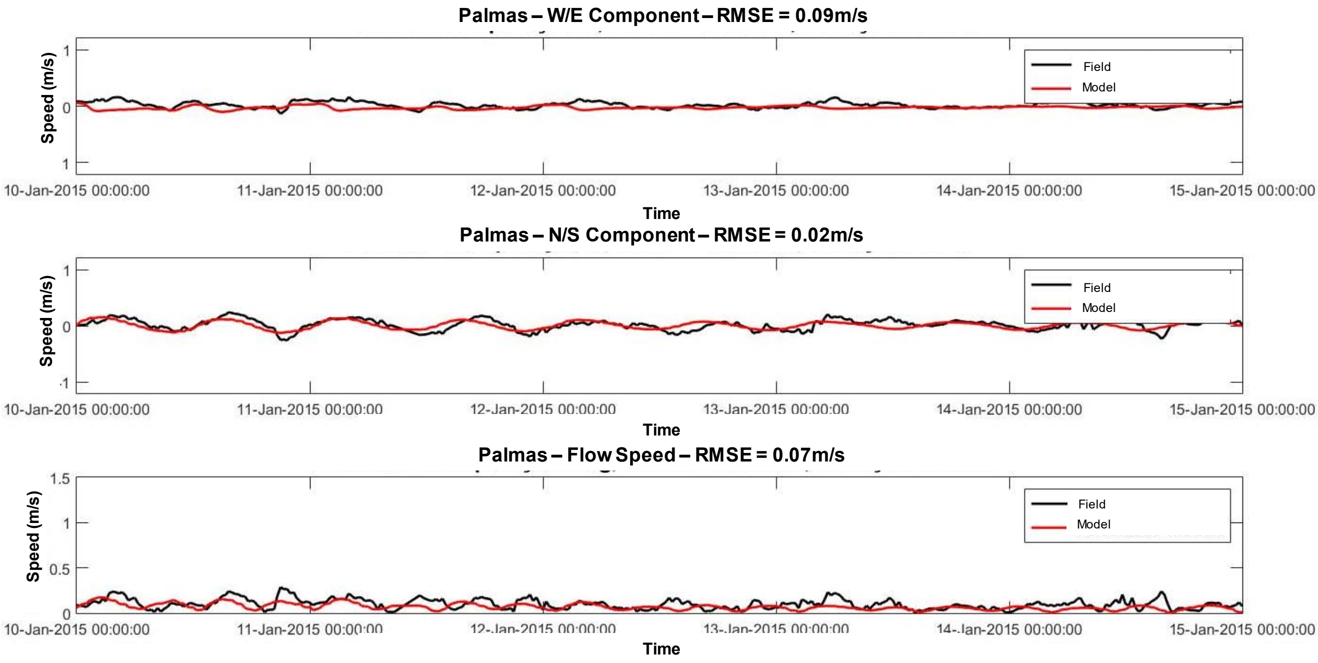

Figure 9. Field X Model Comparison - Current Speed – Palmas

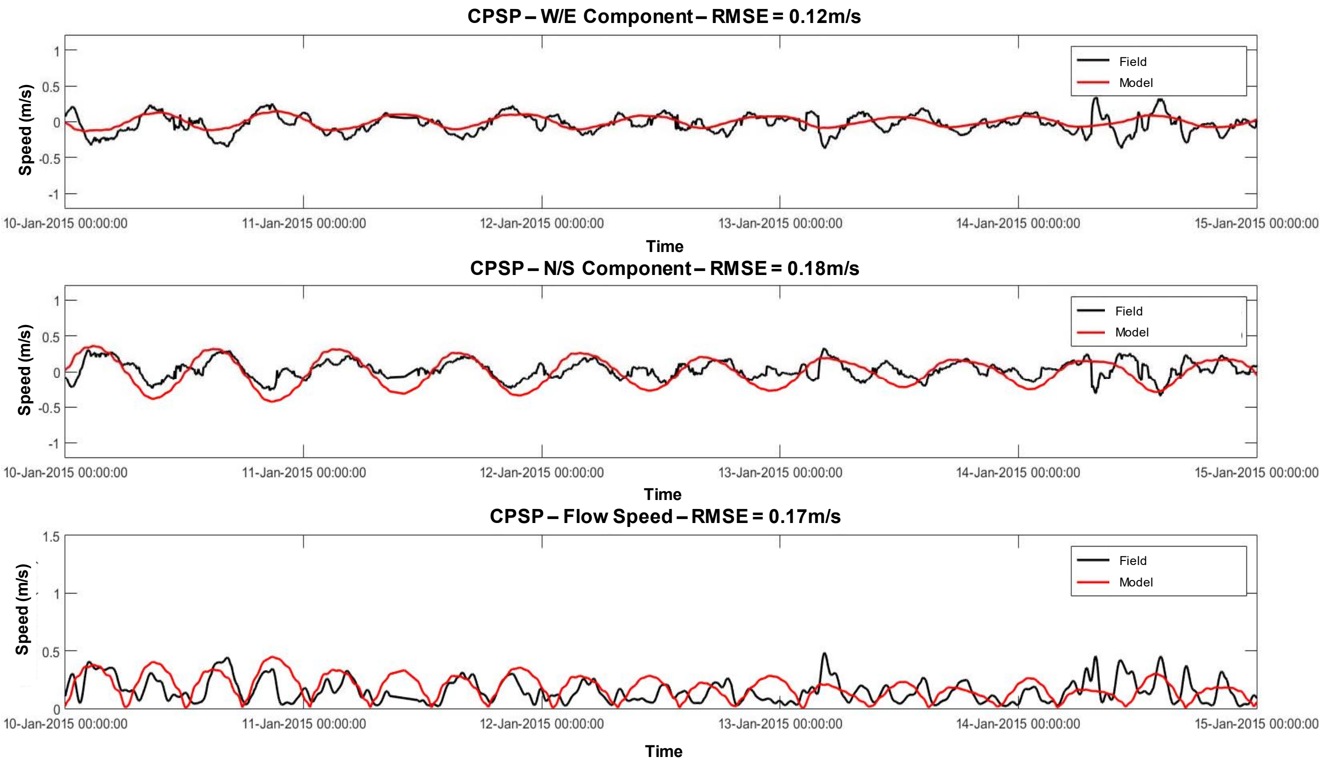

Figure 10. Field X Model Comparison - Current Speed – CPSP

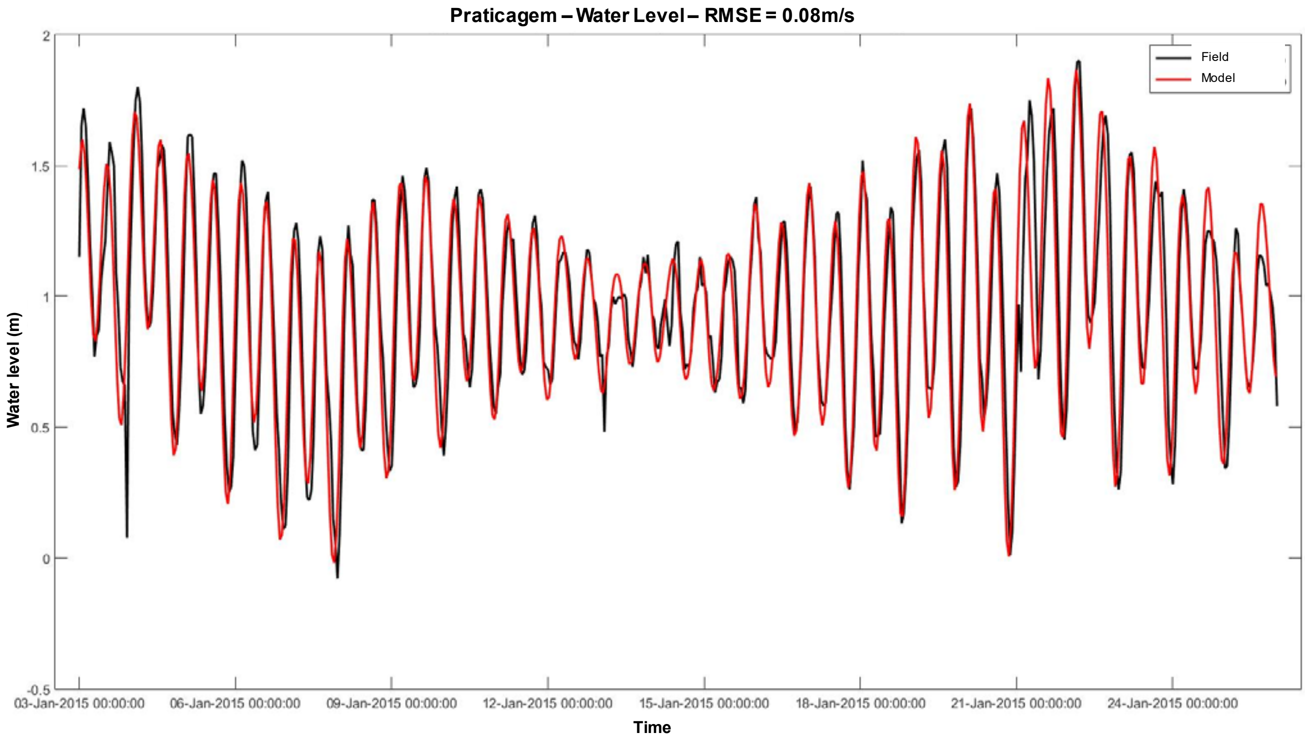

Figure 11. Field X Model Comparison – Water level – Praticagem

Sediment transport model accuracy was evaluated by comparing suspended sediment concentration measured within Santos estuary by DHI (2008) in March 2006. This data was collected along the whole access channel, extending up to the inner area of the estuary, in 11 different sections. Suspended sediment concentration measured within Santos estuary varies between 0.005 kg/m³ and 0.06 kg/m, where 0.02 kg/m³ is the average suspended sediment concentration. Figure 12 shows a comparison between field measurements and modeled data for the mentioned period, indicating the good relation between model and reality. Unfortunately, there were no consecutive bathymetric surveys performed in periods without dredging activities available at the access channel, in order to obtain an ideal calibration of morphological updating.

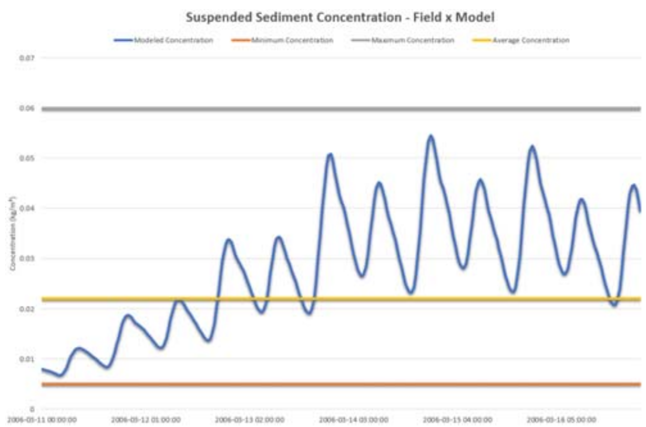

Figure 12. Field X Model Comparison - Suspended Sediment Concentration

5 SIMULATIONS PERFORMED

In order to represent summer and winter period, two different environmental scenarios were selected for simulation performance. The adopted scenarios definition was based on wave statistics analysis, which aimed to select a summer and a winter month that could best represent average wave condition for each period. Figure 13 and Figure 14 expose selected wave conditions for summer and winter periods simulations. Also, for the summer month simulation, river flow condition was considered to be maximum, while average river discharge was considered for a winter month.

Monthly simulations were performed to save computational time. The estimative of annual dredging volumes was simplified by considering six typical months of winter and six typical months of summer. The environmental scenarios were simulated for each design depth: current bathymetry, 15, 16 and 17m.

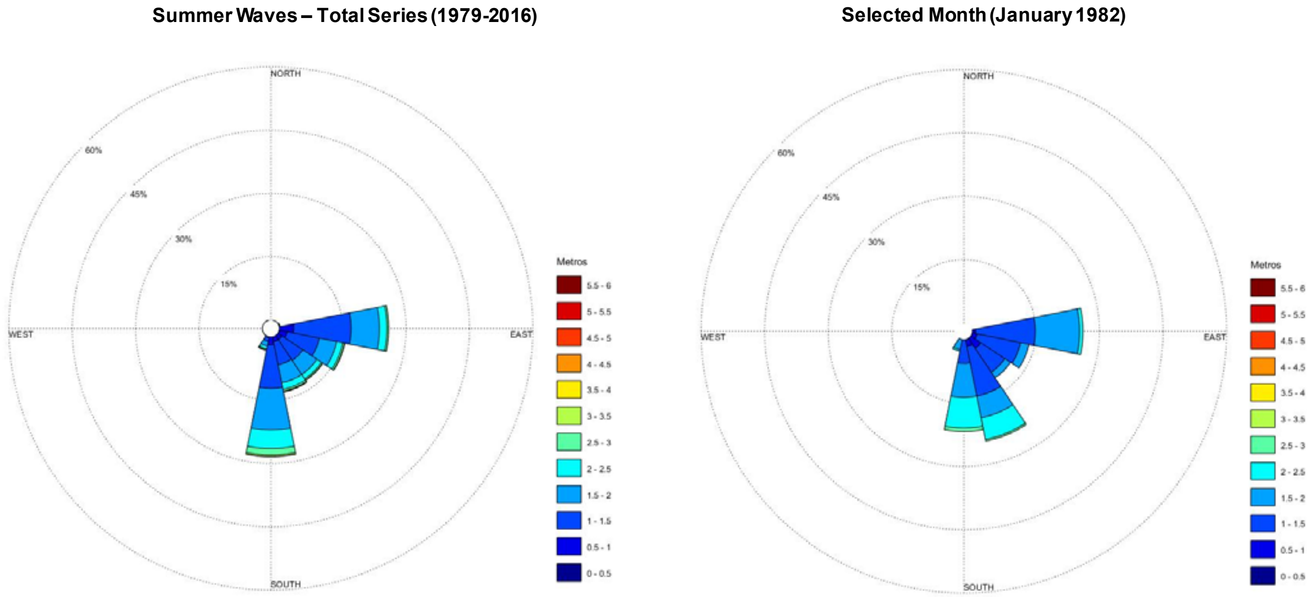

Figure 13 - Selected Summer Period

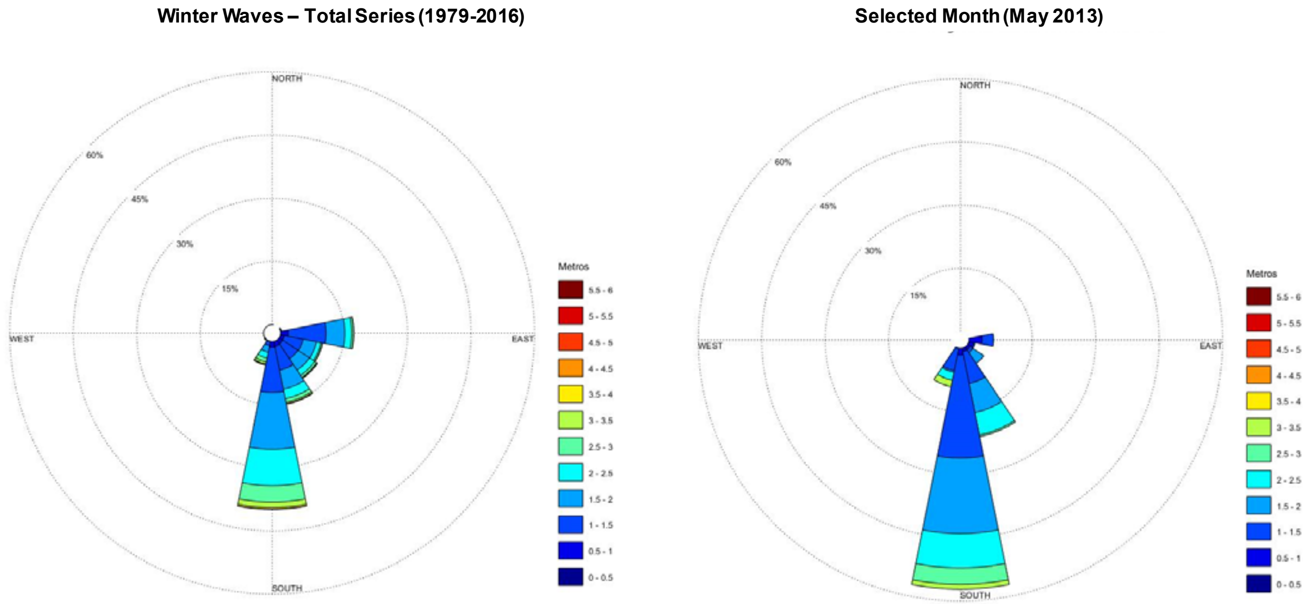

Figure 14 - Selected Winter period

6 RESULTS AND DISCUSSION

6.1 *Current access channel situation*

Figure 15 presents model results of monthly winter and summer simulations and Figure 16 shows the annual sediment deposition distribution in each access channel area.

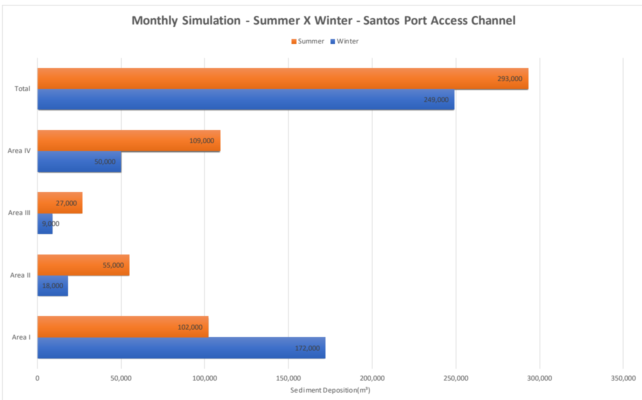

Figure 15. Sediment deposition at Santos Port Access Channel - Summer X Winter

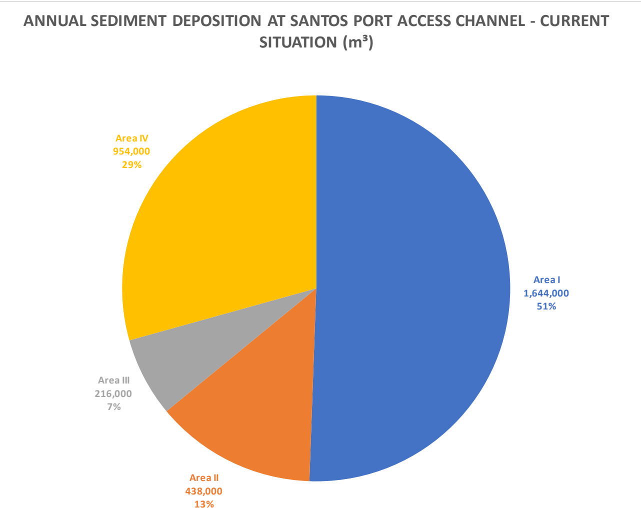

Figure 16. Annual sediment deposition distribution at Santos Port Access Channel

Considering current bathymetry, modeling results indicated that there is an average sediment deposition of about 3,250,000 m³ in the Santos Port Access Channel. About 51% of total sediment accumulation is observed in Area 1, predominantly in the winter period, when wave action is more intense. Withal, in the summer period, sediment deposition occurs predominantly in the inner areas of the access channel, mainly in Area IV, the closer to rivers outfalls. In Areas II and III, sediment deposition rate is lower, due to higher current speeds caused by confined flow.

According to Alfredini (2004), average annual dredging volume between 1978 and 2002 was about 2,500,000 m³ (in situ). Regarding that, after this period, the channel was deepened, it is possible to assume that the model estimative is consistent with reality. Still, when analyzing only Areas II, III and IV, which are not subjected to wave action, 70% of sediment deposition is observed in the summer period, following the rainfall regime of Santos region.

The relation between dredged volumes inside cistern and dredged volumes in situ is about 1.33 for Santos Port Access Channel (Alfredini, 2004). Therefore, according to simulations results, in order to maintain current depths, annual dredging volume shall be about 4,325,000 m³.

6.2 *Design depths comparison*

Figure 17 exposes the model results for annual sediment deposition considering design depths of 15, 16 and 17m (CD) for each area of the Santos Port Access Channel.

The model results indicate that sediment deposition is expected to increase 15%, 55% and 80%, considering channel deepening for 15, 16 and 17m, respectively. A higher increase of sediment deposition is expected to occur in Area I, where was observed an increase up to 140% when the channel was deepened to 17 m (CD). Less increase was observed in Areas II and III, where higher current speeds prevent sediment settling.

Table 1 summarizes modeled results for each design depth.

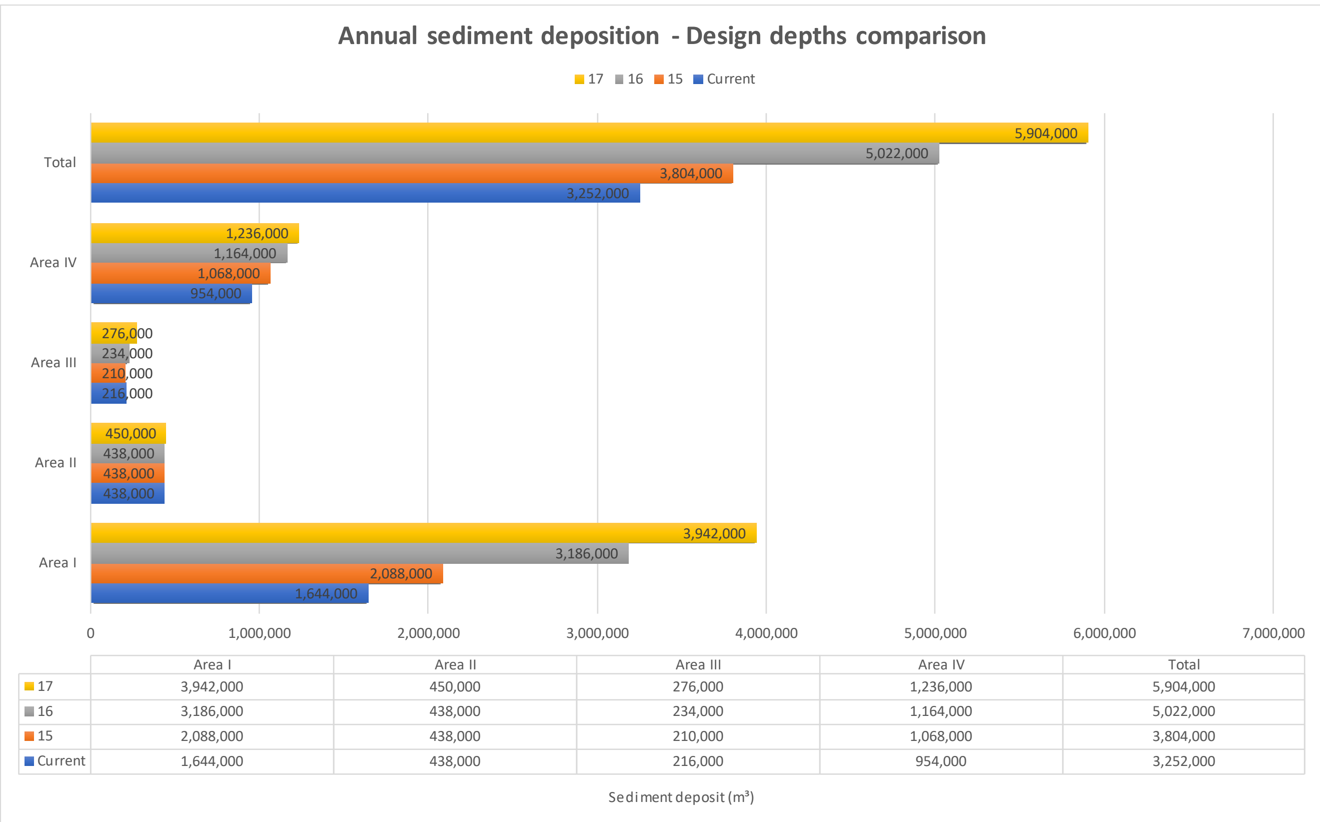

Figure 17. Annual Sediment Deposition – Design depths comparison

Table 1. Annual sediment deposition and dredging prediction for each design depth

Design Depth	Annual Sediment Deposition (m^3)	Annual Dredging Volumes (m^3)	Increase (%)
Current Depth	3,252,000	4,325,000	-
15 m	3,804,000	5,059,000	15%
16 m	5,022,000	6,679,000	55%
17 m	5,904,000	7,852,000	80%

7 CONCLUSIONS

Santos Port is the most important hub port in Latin America and one of the most important ports worldwide. Responsible for 25% of Brazilian balance of trade, it is also the main source of incomes of the city, thereafter heavily contributing for employment generation. Therefore, maintaining and improving the harbor conditions in order to attend the requirements for allowing the entrance of larger vessels is essential to keep the port economic attractiveness. In this context, capital and maintenance dredging stand out as indispensable activities, although they had been neglected and poorly managed during Santos Port history.

The study hereby presented aimed to provide an estimative of sediment deposition and annual average maintenance dredging volumes for different conditions of the Santos Port Access Channel, through hydrodynamic and morphological numerical model simulations of the main environmental scenarios. Although the dataset used for model calibration can be considered incomplete for obtaining proper accuracy, the results presented good relation with reality, representing overall main sediment deposition tendencies in the different areas of the access channel.

The model indicates that, in order to maintain the access channel current depth (March 2016), an annual maintenance dredging volume of about 4,325,000 m^3 is necessary. For deeper design depths, such as 15, 16 and 17 m (CD), increases of 15%, 55%, and 80%, respectively, are expected.

It is remarkable that, in addition to dredging volumes forecast, it is necessary to financially evaluate best design depth for the access channel, considering international economic scenario and vessels' size demand. Also, whereas that deepening the channel implies in a significant increase of sediment deposition, it can be economically or operationally impracticable to maintain the aimed design depth without any structural intervention, such as parallel jetties, which could improve access channel maintenance by tidal scour.

REFERENCES

Alfredini, P. 2004. Estudo sobre avaliação das taxas de evolução do fundo do canal de acesso ao Porto de Santos no período de 1997 a 2003. Technical Report.

CHM. 2016. Centro de Hidrografia da Marinha – Cartas Náuticas disponíveis. http://www.mar.mil.br/dhn/chm/box-cartas-raster/raster_disponiveis.html

DELTARES. 2014. *Delft 3D-FLOW- Simulation of multi-dimensional hydrodynamic flows and transport phenomena, including sediments*. User Manual. 712p. Delft.

DHI, 2008. Porto de Santos – Modelagem do Transporte de Sedimentos. Technical Report.

Fredsoe, J. 1984. Turbulent boundary layer in wave-current interaction. Journal of Hydraulic Engineering 110: 1103-1120.

Fundação Ricardo Franco. 2008. EIA da Dragagem de Aprofundamento do Canal de Navegação, Bacias de Evolução e Berços de Atracação do Porto Organizado de Santos.

Partheniades, E. 1965. Erosion and Deposition of Cohesive Soils. Journal of the Hydraulics Division, ASCE 91: 105-139.

Van Rijn, L. C. 1993. Principles of Sediment Transport in Rivers, Estuaries and Coastal Seas. Aqua Publications, The Netherlands.

Versteeg, H. K.; Malalasekera, W. 2007. An Introduction to Computational Fluid Dynamics – The Finite Volume Method. Harlow, England: Pearson Education, 517p.